Universiteit
Leiden
The Netherlands

Quantitative systems pharmacology modeling of biotherapeutics in oncology

Betts, A.M.

Citation

Betts, A. M. (2021, June 3). *Quantitative systems pharmacology modeling of biotherapeutics in oncology*. Retrieved from https://hdl.handle.net/1887/3176516

Version:	Publisher's Version
License:	Licence agreement concerning inclusion of doctoral thesis in the Institutional Repository of the University of Leiden
Downloaded from:	https://hdl.handle.net/1887/3176516

Note: To cite this publication please use the final published version (if applicable).

Cover Page

Universiteit Leiden

The handle http://hdl.handle.net/1887/3176516 holds various files of this Leiden University dissertation.

Author: Betts, A.M.
Title: Quantitative systems pharmacology modeling of biotherapeutics in oncology
Issue date: 2021-06-03

Section III.
Modeling of antibody drug conjugates

Chapter 3

Establishing in vitro–in vivo correlation for antibody drug conjugate efficacy:

a PK/PD modeling approach

Dhaval K. Shah, Frank Loganzo, Nahor Haddish-Berhane, Sylvia Musto, Hallie S. Wald, Frank Barletta, Judy Lucas, Tracey Clark, Steve Hansel, Alison Betts

Journal of Pharmacokinetics and Pharmacodynamics 45(2): 339-349 (2018).

3.1 Abstract

The objective of this manuscript was to establish in vitro–in vivo correlation (IVIVC) between the in vitro efficacy and in vivo efficacy of antibody drug conjugates (ADCs), using a PK/PD modeling approach. Nineteen different ADCs were used to develop IVIVC. In vitro efficacy of ADCs was evaluated using a kinetic cell cytotoxicity assay. The cytotoxicity data obtained from in vitro studies was characterized using a novel mathematical model, parameter estimates from which were used to derive an in vitro efficacy matrix for each ADC, termed as 'in vitro tumor static concentration' ($TSC_{in\ vitro}$). $TSC_{in\ vitro}$ is a theoretical concentration at continuous exposure of which the number of cells will neither increase nor decrease, compared to the initial cell number in the experiment. The in vivo efficacy of ADCs was evaluated using tumor growth inhibition (TGI) studies performed on human tumor xenograft bearing mice. The TGI data obtained from in vivo studies was characterized using a PK/PD model, parameter estimates from which were used to derive an in vivo efficacy matrix for each ADC, termed as 'in vivo tumor static concentration' ($TSC_{in\ vivo}$). $TSC_{in\ vivo}$ is a theoretical concentration if one were to maintain in the plasma of a tumor bearing mouse, the tumor volume will neither increase nor decrease compared to the initial tumor volume. Comparison of the $TSC_{in\ vitro}$ and $TSC_{in\ vivo}$ values from 19 ADCs provided a linear and positive IVIVC. The Spearman's rank correlation coefficient for $TSC_{in\ vitro}$ and $TSC_{in\ vivo}$ was found to be 0.82. On average $TSC_{in\ vivo}$ was found to be ~ 27 times higher than $TSC_{in\ vitro}$. The reasonable IVIVC for ADCs suggests that in vitro efficacy data was correctly able to differentiate ADCs for their in vivo efficacy. Thus, IVIVC can be used as a tool to triage ADC molecules in the discovery stage, thereby preventing unnecessary scaling-up of ADCs and waste of time and resources. An ability to predict the concentration of ADC that is efficacious in vivo using the in vitro data can also help in optimizing the experimental design of preclinical efficacy studies. As such, the novel PK/PD modeling method presented here to establish IVIVC for ADCs holds promise and should be evaluated further using diverse set of cell lines and anticancer agents.

3.2 Introduction

In vitro cytotoxicity assay and murine models of human tumor xenograft are the most widely used experimental systems in the discovery and preclinical development of oncology drugs. The routinely used in vitro cytotoxicity assays (usually performed in a 96-well plate format) not only provides a high throughput way to triage anticancer molecules in the discovery setting, but also provide a point estimate of a given molecule's potency for the chosen cell line i.e. IC50 or IC90. The human tumor xenografts transplanted into immune-compromised mice are the regularly used preclinical animal models to evaluate the efficacy of novel anticancer agents in vivo. These animal models not only help triage molecules based on their integrated pharmacokinetics (PK) and potency profile, but also provide some quantification of a given molecule's potency for inhibiting tumor growth in a given xenograft model (e.g. T/C ratio). Although both of these experimental approaches, i.e. in vitro cytotoxicity assay and murine tumor xenografts, are very informative in their own ways to help define a drug's potency and efficacy; there are only a handful of reports which have integrated the information from these two systems to establish in vitro-in vivo correlation (IVIVC) for the efficacy of chemotherapeutic drugs.

One of the reasons for the lack of efforts in establishing IVIVC for anticancer drug efficacy may be the different efficacy matrix that both the in vitro and the in vivo systems provide. The results from in vitro cytotoxicity assays are processed to usually represent the efficacy of a drug in the form of ICx (i.e. the concentration of the drug that causes X% reduction in the cell viability of the treatment group compared to the control group), at a certain period of time after the start of the treatment. Whereas the results from the in vivo tumor growth inhibition (TGI) studies are usually processed to provide the efficacy of a drug in the form of either minimum efficacious dose (MED), area under the drug concentration-time curve (AUC) at MED, or T/C ratio. Thus, because of the different units used to express the efficacy, it would be very difficult to compare the efficacy parameters obtained from an in vitro experimental system to the ones obtained from an in vivo system. This manuscript strives to demonstrate the use of pharmacokinetic-pharmacodynamic (PK/PD) modeling approach to derive a comparable efficacy parameter from the in vitro and in vivo experimental systems, in order to help establish IVIVC for the efficacy of anticancer drugs, using antibody drug conjugates (ADCs) as model therapeutic agents.

Here we have evaluated the in vitro cytotoxicity of 19 different ADCs using a kinetic cytotoxicity assay [1], where the viability of cancer cells was determined at multiple time points after incubation with various concentrations of ADCs. The viable cell number vs. time profile obtained from in vitro experiments was fitted by a semi-mechanistic PK/PD model to derive the secondary parameter for IVIVC, tumor static concentration (TSC). The TSC value derived from in vitro kinetic cytotoxicity assay ($TSC_{in\ vitro}$) is a theoretical concentration of the drug in a cell culture well, at continuous exposure of which the number of viable cells in the well will neither increase nor decrease compared to the starting cell number. To enable in vivo PK/PD modeling, the PK of all 19 ADCs that were tested in vitro, was determined in mice. A multiple dose TGI study was conducted for each of the 19 ADCs, in a murine human tumor xenograft model developed using the same cell line that was used for the in vitro cytotoxicity assay. The TGI data was modeled using a semi-mechanistic PK/PD model, and TSC was derived from the estimated parameters. The TSC value derived from TGI data ($TSC_{in\ vivo}$) is the theoretical concentration of a drug if one were to maintain in the plasma of a tumor bearing mouse, the tumor volume will neither increase nor decrease compared to the initial tumor volume of the experiment. The $TSC_{in\ vitro}$ and $TSC_{in\ vivo}$ values derived for each ADC were correlated to help establish the IVIVC for the efficacy of ADCs.

3.3 Methods

In vitro kinetic cytotoxicity assay

Her2 expressing N87 gastric carcinoma cells were seeded into 96-well cell culture plates for 24 hours before the ADC treatment. Cells were treated with 10 different 3-fold serially diluted ADC concentrations in duplicate. Replicate plates of treated cells were incubated for 1, 2, 3, 6, and 8 days to obtain time-course of drug effect. On the specified harvest day, 30 µl of Cell Titer Glo® One Solution Assay reagent (Promega Cat # G3581) was added to the cells and incubated for 0.5 hours at room temperature while shaking and protecting from light. After incubation, the luminescence was measured on a Victor plate reader (Perkin Elmer, Waltham, MA). Relative cell viability was determined as percentage of untreated control. In a parallel set of plates, a linear

standard curve of N87 cell number vs. relative luminescence units (RLU) was generated to convert the RLU of experimental samples into cell number for kinetic analyses.

Modeling the in vitro cytotoxicity data

The viable cell number versus time profiles obtained from in vitro kinetic cytotoxicity assays was modeled using the semi-mechanistic PK/PD model displayed in Figure-1. The PD model used here is developed by combining the two widely used mathematical models for characterizing the efficacy of chemotherapeutic drugs, the signal distribution model developed by Lobo and Balthasar [1] and the cell distribution model developed by Simeoni *et al.* [2,3]. As described in Figure-1, the model assumes that the presence of drug in the cell culture well ($C_{in\ vitro}$) initiates a concentration dependent nonlinear killing signal ($K1_{kill}$), which imparts its effect on cancer cells ($K4_{kill}$) following a transduction delay characterized by Tau_S. In the absence of drug, the cells are allowed to grow exponentially (K_g) until they reach a plateau ($Cell_{Maximum}$). Once the growing cancer cells in the well responds to the killing signal ($K4_{kill}$), a part of them is shuttled to the non-growing cell compartments, from where the cells are destined to die following a transduction delay characterized by Tau_C. The model equations are provided below:

$$\frac{dK1_{kill}}{dt} = \frac{1}{Tau_S} \bullet \left(\frac{K_{max\_in\_vitro} \bullet C_{in\_vitro}^{\gamma}}{IC_{50\_in\_vitro}^{\gamma} + C_{in\_vitro}^{\gamma}} - K1_{kill} \right) ;\ IC = 0 \quad (1)$$

$$\frac{dK2_{kill}}{dt} = \frac{1}{Tau_S} \bullet (K1_{kill} - K2_{kill}) ;\ IC = 0 \quad (2)$$

$$\frac{dK3_{kill}}{dt} = \frac{1}{Tau_S} \bullet (K2_{kill} - K3_{kill}) ;\ IC = 0 \quad (3)$$

$$\frac{dK4_{kill}}{dt} = \frac{1}{Tau_S} \bullet (K3_{kill} - K4_{kill}) ;\ IC = 0 \quad (4)$$

$$\frac{dCell_1}{dt} = Kg \bullet \left(1 - \frac{Cell_{Total}}{Cell_{Maximum}}\right) \bullet Cell_1 - K4_{kill} \bullet Cell_1 ;\ IC = Cell_{initial} \quad (5)$$

$$\frac{dCell_2}{dt} = K4_{kill} \bullet Cell_1 - \frac{1}{Tau_C} \bullet Cell_2 ;\ IC = 0 \quad (6)$$

$$\frac{dCell_3}{dt} = \frac{1}{Tau_C} \bullet (Cell_2 - Cell_3) ;\ IC = 0 \quad (7)$$

$$\frac{dCell_4}{dt} = \frac{1}{Tau_C} \bullet (Cell_3 - Cell_4) ;\ IC = 0 \quad (8)$$

$$Cell_{Total} = Cell_1 + Cell_2 + Cell_3 + Cell_4 \quad (9)$$

Above, $K1_{kill}$, $K2_{kill}$, $K3_{kill}$ and $K4_{kill}$ are the killing signal compartments, and $Cell_1$, $Cell_2$, $Cell_3$, and $Cell_4$ are the cell number compartments. $K_{max\_in\_vitro}$ is the maximum rate at which the drug can kill the cells and $IC_{50\_in\_vitro}$ is the drug concentration at which the kill rate is half of the maximum. IC refers to initial conditions of the differential equations.

The viable cell number versus time profiles generated for the control and all the concentration groups of a given ADC were fitted simultaneously by the model, using the naïve pool approach in the software Monolix® (v3.2, Paris, France - SAEM algorithm). For all the fittings the slope

coefficient γ was fixed to 1 and the residual error was described using the constant error model. The $TSC_{in\ vitro}$ value for each compound was calculated using the following equation, which is derived from the equation 5:

$$TSC_{in\ vitro} = \frac{Kg \bullet IC_{50\_in\_vitro}}{K_{max\_in\_vitro} - Kg} \quad (10)$$

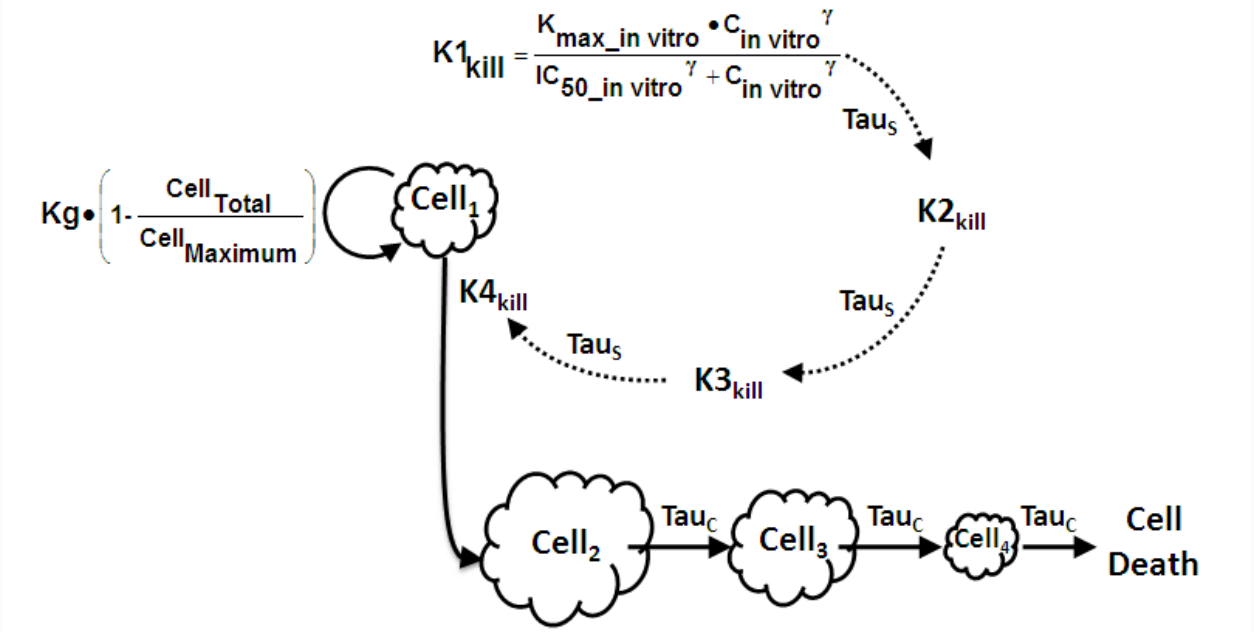

Figure 1: A schematic diagram demonstrating the mathematical model used to characterize in vitro kinetic cytotoxicity data. Please refers to the '*Modeling the In Vitro Cytotoxicity Data*' subsection in the '*Methods*' section for more details about the symbols and structure of the model.

Mouse PK of ADCs

All procedures using mice were approved by the Pfizer Institutional Animal Care and Use Committees and conducted according to established Animal Use Protocols. Female athymic (nu/nu) mice, 6-8 weeks of age, were obtained from Charles River Laboratories (Wilmington, MA) and housed in the vivarium at Pfizer Inc, Pearl River, NY. Mouse blood (10 µL) was collected serially from mice (n=3) for up to 336 h after a single 3 mg/kg dose of each ADC. Quantitation of the ADC concentrations in mouse plasma was achieved using ligand binding assays (ELISA or Gyros Immunoassay). In general, ADC was captured using a commercial polyclonal Anti-Human IgG (Fc specific) antibody, and the bound ADC was detected using a biotinylated polyclonal anti-payload antibody (Pfizer, Inc.). The limit of quantitation (LOQ) for the ligand binding assays was 80-100 ng/mL.

The plasma concentration vs. time profiles of each ADC in mouse was characterized using a two compartmental model with linear clearance from the central compartment. The model equations are provided below:

$$\frac{dX1_{ADC}}{dt} = -\frac{CL_{ADC}}{V1_{ADC}} \bullet X1_{ADC} - \frac{CLD_{ADC}}{V1_{ADC}} \bullet X1_{ADC} + \frac{CLD_{ADC}}{V2_{ADC}} \bullet X2_{ADC}; IC = Dose_{ADC} \quad (11)$$

$$\frac{dX2_{ADC}}{dt} = \frac{CLD_{ADC}}{V1_{ADC}} \bullet X1_{ADC} - \frac{CLD_{ADC}}{V2_{ADC}} \bullet X2_{ADC}; IC = 0 \quad (12)$$

Above, $X1_{ADC}$ and $X2_{ADC}$ are the amount of ADC in the central and peripheral compartment. $V1_{ADC}$ and $V2_{ADC}$ are the ADC volumes of distribution in the central and peripheral compartment. CL_{ADC} is the clearance of ADC from the central compartment and CLD_{ADC} is the distributive clearance between the central and peripheral compartments (see Fig 2). The model was fitted to the data using the weighting scheme of $1/(Y\hat{})^2$, by the software WinNonlin (version 5.2, Pharsight Corp., Mountain View, CA). Here Y^ refers to model predicted concentrations.

TGI studies in mouse xenografts

All procedures using mice were approved by the Pfizer Institutional Animal Care and Use Committees and conducted according to established Animal Use Protocols. Female athymic (nu/nu) mice, 6-8 weeks of age, were obtained from Charles River Laboratories (Wilmington, MA) and housed in the vivarium at Pfizer Inc, Pearl River, NY. Mice were injected subcutaneously with ~7.5 million N87 (gastric cancer cell line) tumor cells in 50% matrigel and the tumor was allowed to grow. Once the tumor volume reached 200-400 mm^3, animals were divided into 4 groups (6 to 10 mice per group) for each ADC. Animals were intravenously administered with saline (vehicle group) or ADC at 1,3 and 10 mg/kg dose levels (treatment groups), at the dosing regimen of Q4d x 4 starting on Day 1 after the randomization. All ADCs were dosed based on antibody (mAb) content. Tumors were measured at least once a week up to at least 41 days after dosing. The tumor volume was calculated using the following formula: Tumor volume in mm^3 = 0.5 x (tumor $width^2$) × (tumor length) [4]. The LOQ for the tumor measurement was 40 mm^3.

Modeling the TGI Data

The tumor volume vs. time data obtained from TGI studies was fitted using the PK/PD model displayed in Figure-2. As mentioned in the '*Mouse PK of ADCs*' section, the plasma PK of ADC was characterized using the standard 2 compartment model with linear elimination from the central compartment. The PD effect of ADC was characterized using a semi-mechanistic (modified cell distribution) model, which we have published earlier [5,6]. Equations for the PD model are provided below:

$$\frac{dV1}{dt} = \frac{k_{g_{Exponential}} \bullet \left(1 - \frac{TV}{V_{Max}}\right) \bullet V1}{\left(1 + \left(\frac{k_{g_{Exponential}}}{k_{g_{Linear}}} \bullet TV\right)^{\psi}\right)^{1/\psi}} - \frac{k_{kill\_Max} \bullet C_{ADC}}{KC_{50} + C_{ADC}} \bullet V1 \; ; IC = V_{Initial} \quad (13)$$

$$\frac{dV2}{dt} = \frac{k_{kill\_Max} \bullet C_{ADC}}{KC_{50} + C_{ADC}} \bullet V1 - \frac{V2}{Tau}\ ; IC = 0 \quad (14)$$

$$\frac{dV3}{dt} = \frac{(V2 - V3)}{Tau}; IC = 0 \quad (15)$$

$$\frac{dV4}{dt} = \frac{(V3 - V4)}{Tau}; IC = 0 \quad (16)$$

$$TV = V1 + V2 + V3 + V4 \quad (17)$$

Above, V1 is the growing tumor volume compartment whereas V2, V3, V4 are the non-growing tumor volume transit compartments. TV is the total tumor volume and $V_{initial}$ is the initial tumor volume. The tumor growth function is adapted from Simeoni *et al.* [2], where initially the tumor is allowed to grow according to an exponential growth rate $k_{gExponential}$ that switches to the linear growth rate $k_{gLinear}$ based on the total tumor volume and switching coefficient ψ. In order to account for the plateau observed at higher tumor volumes, a saturation function was added to the tumor growth term used by Simeoni *et al.* C_{ADC} is the ADC concentration in the plasma, k_{kill_Max} is the maximum rate at which the drug can kill the tumor, and KC_{50} is the drug concentration at which the kill rate is half of the maximum. The transit delay between the non-growing tumor compartments is described by Tau.

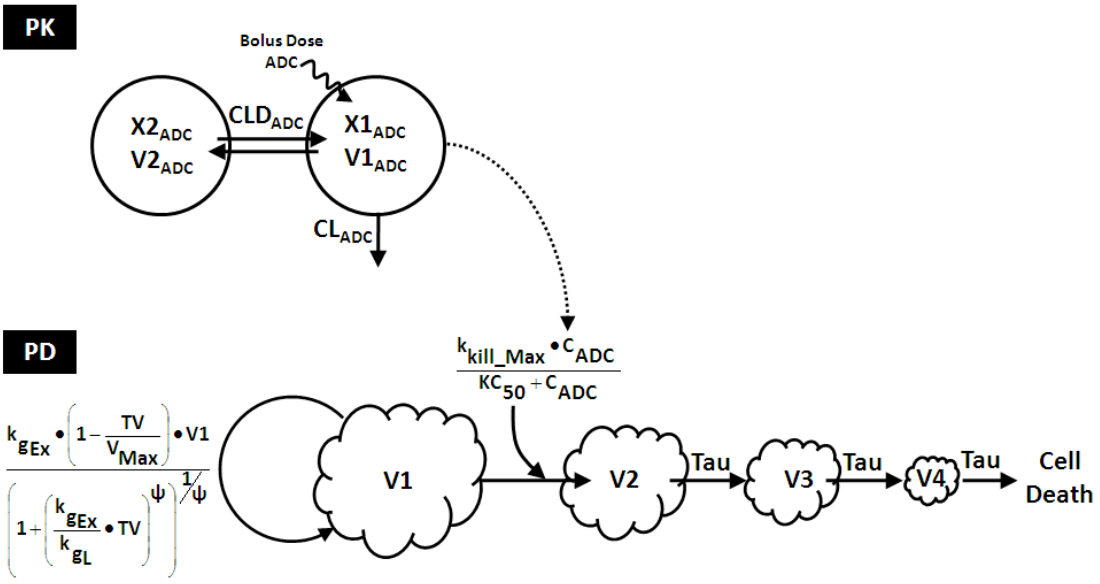

Figure 2: The PK/PD model used to characterize the TGI data for ADCs. Please refers to the '*Modeling the TGI Data*' subsection in the '*Methods*' section for more details about the symbols and structure of the model.

In order to fit the PK/PD model to TGI data generated for each ADC, a sequential parameter estimation method was followed, where the PK parameters were first estimated using the naïve pooling approach and then they were fixed to estimate the PD parameters using the population approach. This two-stage approach was preferred over the joint population PK/PD approach because the detailed information about the PK of ADC in each animal involved in the PD study

was not available. While estimating the PD parameters, initially the tumor growth parameters and inter-individual variability (IIV) for them were estimated from just the control group data. Subsequently, the IIV of the growth parameters and V_{max} were fixed, followed by estimation of both the growth and drug effect parameters simultaneously using the software Monolix® (v3.2, Paris, France - SAEM algorithm). The residual error was characterized using additive, proportional or, additive + proportional error models. The quality of the model fittings was assessed by considering weighted residual plot, observations against individual predictions (iPRED) and population predictions (PRED) plots, AIC and BIC values, and confidence in the parameter estimates (i.e. CV%).

The $TSC_{in\ vivo}$ value for each compound was calculated using the following equation, which is derived from the equation 13:

$$TSC_{in_{vivo}} = \frac{k_{g_{Exponential}} \bullet KC_{50} \bullet \left(1 - \frac{V_{initial}}{V_{max}}\right)}{k_{kill_{Max}} \bullet \left(1 + \left(\frac{k_{g_{Exponential}}}{k_{gLinear}} \bullet V_{initial}\right)^{\varphi}\right)^{\frac{1}{\varphi}} - k_{g_{Exponential}} \bullet \left(1 - \frac{V_{initial}}{V_{max}}\right)} \quad (18)$$

Equation 18 can be further simplified by considering whether $\left(\frac{k_{g_{Exponenial}}}{k_{g_{Linear}}} \bullet V_{Initial}\right)$ is ≤1 or >1. If $\left(\frac{k_{g_{Exponenial}}}{k_{g_{Linear}}} \bullet V_{Initial}\right)$ is ≤1 equation 18 reduces to:

$$TSC_{in\_vivo} = \frac{k_{g_{Exponential}} \bullet KC_{50}}{k_{kill\_Max} - k_{g_{Exponential}}} \quad (19)$$

and if $\left(\frac{k_{g_{Exponential}}}{k_{g_{Linear}}} \bullet V_{Initial}\right)$ is >1 equation 18 reduces to:

$$TSC_{in\_vivo} = \frac{k_{g_{Linear}} \bullet KC_{50}}{k_{kill\_Max} \bullet V_{Initial} - k_{g_{Linear}}} \quad (20)$$

Please refer to Haddish-Berhane *et al.* [6] for detailed derivation of abovementioned simplified equations and for the discussion about pathophysiological meaning behind the simplifications.

Establishing IVIVC using $TSC_{in\ vitro}$ and $TSC_{in\ vivo}$

The $TSC_{in\ vitro}$ and $TSC_{in\ vivo}$ values for each ADC was plotted on a scatter plot and observed for any trends or outliers. The data was analyzed to find out the relationship between $TSC_{in\ vitro}$ and $TSC_{in\ vivo}$ and, to determine the Spearman's rank correlation coefficient, since it is a nonparametric statistical test that does not assume normal distribution for variables. The relationship between $TSC_{in\ vitro}$ and $TSC_{in\ vivo}$ was established by fitting the data to the power model, using the software WinNonlin (version 5.2, Pharsight Corp., Mountain View, CA):

$$TSC_{in_{vivo}} = A \bullet TSC_{in_{vitro}}{}^{B}$$

3.4 Results

In Vitro Kinetic Cytotoxicity Assay

A representative in vitro 'cell number vs. time' profile obtained at various concentrations of one of the 19 ADCs (i.e. trastuzumab-DM1 or T-DM1) is displayed in Figure-3A. As shown in the Figure-3A for T-DM1, for most of the ADCs tested, it was observed that the effect of the ADC on cell viability started after a delay of ~1 day. For most of the ADCs the concentration-effect profile was very steep, and the range of concentrations between which the effect of the ADC varied from almost no effect to the maximum effect was very narrow. For example, as shown in the Figure-3A, at the concentration of 0.46 nM the effect of T-DM1 on cell viability was as low as the control group, whereas at the concentration of 4.12 nM the effect was as high as 1000 nM. It was also observed that it took as many as 6 days before the efficacious concentrations of ADC were able to kill most of the cancer cells in the well, suggesting a gradual and not sudden rate of cell death after exposure to ADC's killing signal. Apart from one of the ADCs, all the ADCs were able to kill the cancer cells in the well at the concentration range tested.

Modeling the In Vitro Cytotoxicity Data

Figure-3B shows a representative model fitting of the in vitro 'viable cell number vs. time' data generated using T-DM1, in the form of 'model predicted cell number vs. observed cell number' plot. Representative parameter estimates from the model fitting shown in Figure-3B are provided in the Table-1. The model did a reasonably good job in fitting the data for most of the ADCs, except for one ADC that did not show any killing. Table-3 provides the calculated (using equation 10) $TSC_{in\ vitro}$ values for the 19 ADCs tested. For the ADC that did not show any killing, the TSC value was assumed to be greater than the highest concentration tested i.e. 1000 nM.

Table 1: Parameter estimates obtained from fitting the model shown in Figure-1 to the in vitro 'viable cell number versus time' data generated following T-DM1 treatment.

Parameter	Estimate	% RSE	Unit
Kg	1.05	4	Day^{-1}
$Cell_{Maximum}$	25300	4	Unit less
Tau_C	0.199	43	Day
Tau_S	0.302	9	Day
$K_{max\_in\_vitro}$	1.62	3	Day^{-1}
$IC^{\gamma}_{50\_in\_vitro}$	3.04	8	nM
γ	1	Fixed	Unitless
$TSC_{in\ vitro}$	5.6	Derived	nM

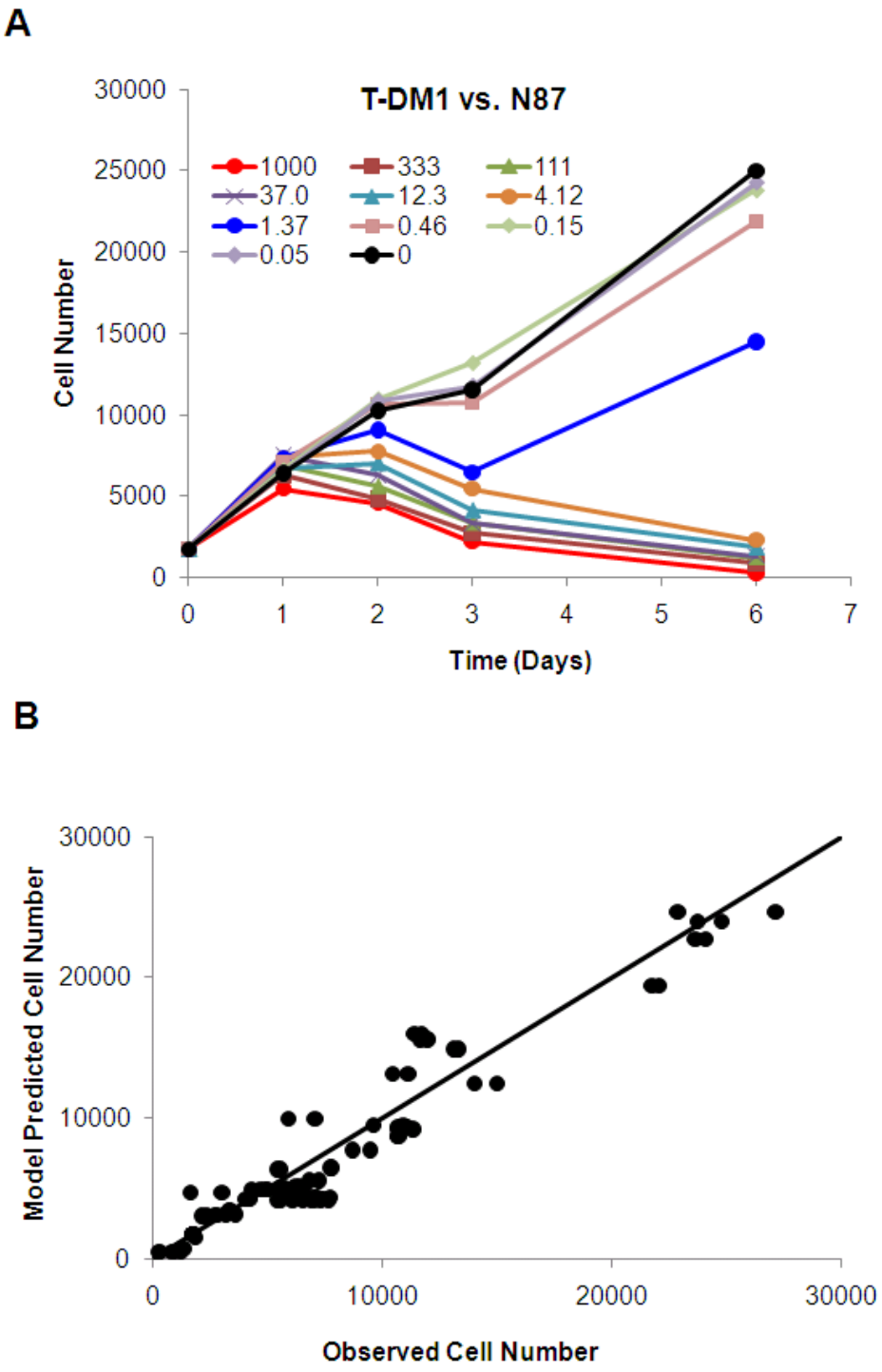

Figure 3: (A) The figure displays 'viable cell number vs. time' profiles generated after incubating different concentrations of Trastuzumab-DM1 with N87 cells. **(B)** The quality of model fitting to the data displayed in the panel A is demonstrated as a plot of 'Model predicted cell number vs. Observed cell number'.

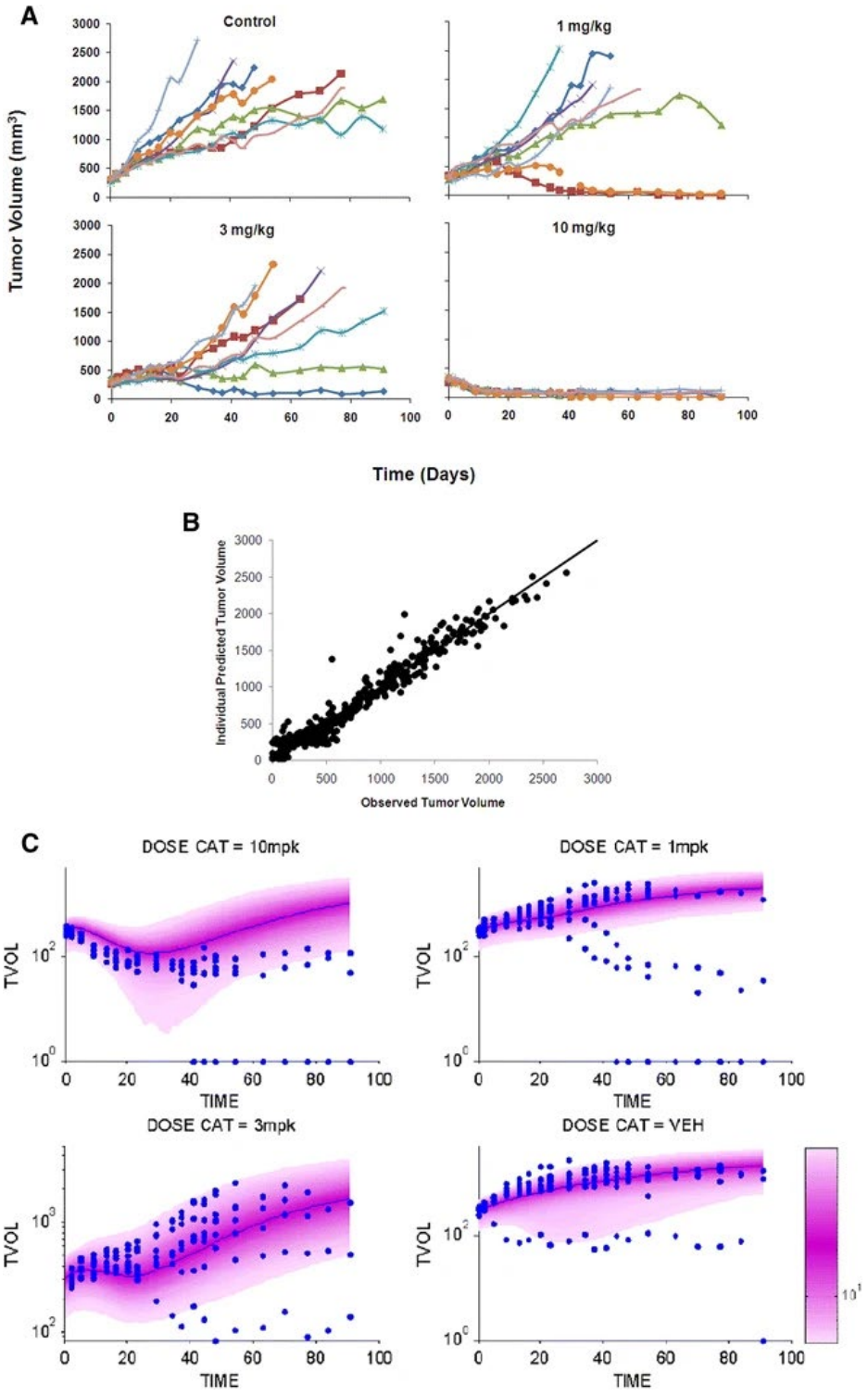

Figure 4: (A) The TGI data obtained after administration of different doses of Trastuzumab-DM1 into N87 xenografts bearing mice. **(B)** The quality of PK/PD model fitting to the TGI data displayed in panel **a** is demonstrated as a plot of 'Individual model predicted tumor volume versus observed tumor volume'. **(C)** The visual predictive check (VPC) for model fitting of T-DM1 TGI data. The symbols represent observed data and the shaded region represent 90% confidence interval

Modeling the Data from TGI Studies in Mouse Xenografts

Figure-4A shows representative tumor volume vs. time profiles obtained from the TGI study conducted in N87 xenografts using one of the ADCs, T-DM1. As demonstrated in the figure for T-DM1, all the ADCs showed a dose dependent response profile. Figure-4B displays the 'observed tumor volume vs. individual predicted tumor volume' profile obtained from the model fitting of the data presented in Figure-4A. Parameter estimates from the model fitting of T-DM1 TGI data are provided in Table-2. As evident from the Figure-4B and Table-2, the model did a reasonably good job in fitting the TGI data for T-DM1. The model also performed well for the characterization of TGI data for all the other ADCs tested (data not shown). The $TSC_{in\ vivo}$ values calculated for T-DM1 and other ADCs, using equations 19 or 20, are reported in Table-3.

Table 2: Parameter estimates obtained from fitting the model shown in Figure-2 to the TGI data generated in N87 xenografts following T-DM1 treatment.

Parameter	Estimate	%RSE	Unit
$k_{g_{Exponenial}}$	0.0732	11	Day^{-1}
$k_{g_{Linear}}$	37.9	17	$mm^3 \bullet Day^{-1}$
V_{Max}	4.22E+03	18	mm^3
Tau	1.36	16	Day
k_{kill_Max}	0.405	38	Day^{-1}
KC_{50}	131	48	µg/mL
ψ	20	Fixed	Unit less
$TSC_{in\ vivo}$	28.9	Derived	µg/mL
$IIV\_k_{g_{Exponenial}}$	0.47	38	Unitless
$IIV\_k_{g_{Linear}}$	0.781	27	Unitless

IIV: interindividual variability

Establishing IVIVC using $TSC_{in\ vitro}$ and $TSC_{in\ vivo}$

Figure-5 depicts the plot generated to correlate $TSC_{in\ vitro}$ and $TSC_{in\ vivo}$, which shows a linear trend between the two variables. The Spearman's rank correlation coefficient between $TSC_{in\ vitro}$ and $TSC_{in\ vivo}$ was found to be 0.82. The ADC that did not show any killing in the in vitro assay (gray symbol in the figure) was considered outlier for building the IVIVC. When this outlier was included for analysis the Spearman's rank correlation coefficient was found to be 0.85. Fitting of the power model to the data (excluding the outlier) that demonstrates a linear and positive relationship between $TSC_{in\ vitro}$ and $TSC_{in\ vivo}$ provided the slope value of 26.8 (CV%=15.2) and an exponent of 0.83 (CV%=9.82); with the weighted correlation coefficient (R^2) value of 0.81.

Table 3: $TSC_{in\ vitro}$ and $TSC_{in\ vivo}$ values derived for each ADC to establish IVIVC.

ADC ID	$TSC_{in\ vitro}$, nM (%RSE)	$TSC_{in\ vivo}$, nM (% RSE)
ADC1	0.23 (9.01)	7.18 (19.5)
ADC2	0.51 (9.31)	11.0 (21.2)
ADC3	0.61 (9.54)	32.7 (11.6)
ADC4	0.62 (9.45)	92.2 (12.3)
ADC5	0.66 (21.2)	14.2 (37.1)
ADC6	0.93 (17.2)	33.5 (34.1)
ADC7	1.12 (12.5)	43.3 (23.1)
ADC8	1.45 (9.66)	41.3 (24.2)
ADC9	2.18 (9.17)	47.9 (57.1)
ADC10	2.56 (20.7)	525 (97)
ADC11	3.10 (17.3)	1160 (63.2)
ADC12	4.08 (15.2)	83.3 (12.1)
ADC13	4.69 (14.1)	135 (144)
ADC14 (Trastuzumab-DM1)	5.60 (16.3)	193 (65.5)
ADC15	12.13 (19)	256 (112)
ADC16	15.26 (11.1)	840 (119)
ADC17	26.25 (29)	441 (71.2)
ADC18	29.64 (19.9)	296 (52.3)
ADC19	> 1000 (NA)	1138 (64.7)

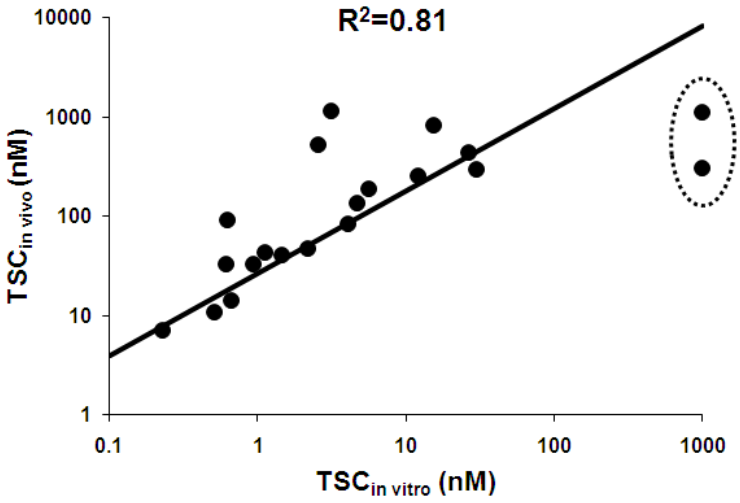

Figure 5: The figure demonstrates the positive linear relationship observed between $TSC_{in\ vitro}$ and $TSC_{in\ vivo}$, which was used to generate the IVIVC. The gray circle highlights the ADC that was an outlier.

3.5 Discussion

IVIVC is generally defined as a predictive mathematical relationship between an in vitro property of the drug and an in vivo response. It is a very routinely sought after and used methodology in the drug discovery and development programs at pharmaceutical industries (e.g. IVIVC between in vitro dissolution and the in vivo absorption rate of a drug from the dosage form). In oncology drug discovery and development programs, scientists have been trying to establish IVIVC between the in vitro sensitivity/resistance of a chemotherapeutic drug and it's in vivo response (preclinical/clinical) [7-10]. However, the majority of these IVIVC studies have based their conclusions on the observation of trends rather than the use of quantitative methods, and most studies have used dichotomous definitions (responsive vs. resistant) of in vitro or in vivo (preclinical/clinical) activity based on largely invalidated cutoff values of efficacy measures [7,10,8,9]. As such, most of the IVIVCs developed for oncology drugs are non-predictive, and overall correlation rates are reported as % of true positive, true negative, false positive, and false negative correlations.

Here we have used mathematical PK/PD modeling to derive a predicative IVIVC between the in vitro and in vivo efficacy of ADCs, which are novel anticancer agents. The success or failure of an effort to establish IVIVC for oncology drugs depend on the quality of experimental models, protocols, and endpoints used to generate the data. Consequently, for our IVIVC study we have conduct a detailed kinetic in vitro and in vivo experiments and have integrated all the available data using mathematical modeling. In the past, a large number of the reported IVIVC are generated using clonogenic in vitro assays that use colorimetric endpoints (e.g. MTT) to infer the

in vitro potency of anticancer drugs (e.g. IC50), and TGI studies in murine xenograft models of human tumors that use changes in tumor volume to infer in vivo potency of the drug (e.g. T/C%). However, the point estimates used for these past IVIVCs do not contain complete information about the time course of a drug's response, and could also change based on the time chosen to determine the particular endpoint (e.g. IC50 and T/C values can be different based on the time point chosen to calculate them). To overcome this issue, we have employed TSC as an integrated endpoint to conduct IVIVC, which is a secondary parameter derived from the model estimates.

While conducting an in vitro time course study to assess the effect of anticancer agents on cell viability is better than a single time point study, correctly integrating the data from the time course study is equally important [10,1]. For example, despite conducting a time course study on the effect of anticancer agents on cell viability, Furukawa *et al.* [10] have reported their data without any kind of integration. This could have been easily accomplished with the use of a mathematical model that can characterize all the data simultaneously [1]. Accordingly, we have not only conducted detailed time course study to investigate the effect of ADCs on cell viability, but we have also integrated all the in vitro data for each ADC simultaneously using a novel mathematical model. The parameter estimates from this model were further used to derive $TSC_{in\ vitro}$. The in vivo efficacy of each ADC was evaluated in xenograft models, where TGI studies were conducted after administering 3 different doses of ADCs, and the data from in vivo studies was integrated using a widely used PK/PD model [2,3]. However, similar to T/C values, just the parameter estimates from the mathematical model cannot be compared with the in vitro results. Thus, $TSC_{in\ vivo}$ was derived from the parameter estimates of the PK/PD model to use it as a variable for correlation with $TSC_{in\ vitro}$.

As reported in Table-3 and Figure-5 and based on the Spearman's rank correlation coefficient value of 0.82, it can be deduced that there was a good positive correlation between $TSC_{in\ vitro}$ and $TSC_{in\ vivo}$. These data suggest that the in vitro studies were correctly able to rank ADCs in terms of in vivo potency. Of note, the estimated value for the ratio of $TSC_{in\ vivo}$ to $TSC_{in\ vitro}$ for all the ADCs was ~27 (the slope of the power model fitted to the linear relationship between $TSC_{in\ vivo}$ and $TSC_{in\ vitro}$), which imply that in order to achieve tumor stasis in vivo ~27 fold higher concentrations of ADC need to be maintained in the plasma of tumor bearing mouse compared to the ADC concentration in the cell culture media. This observation is consistent with the fact that tumor concentrations of antibodies/ADCs can be considerably lower than the plasma concentrations, requiring a higher plasma concentration to achieve tumor concentrations similar to the cell culture media concentration. The IVIVC established in this manuscript can help an ADC discovery and development project team triage the ADCs based on their relative potency and can help the team make go/no-go decisions about a particular ADC based on the expected plasma concentration required to achieve stasis. Thus, the triaging based on IVIVC can save a lot of time, resources, and animals by preventing unnecessary scale-up of ADCs and unnecessary in-vivo experiments. The ability to predict in vivo stasis concentration based on the in vitro experiment can also help scientists design an optimal dosing regimen with suitable doses.

It is important to point out that for conducting IVIVC the same cell line was used for the in vitro and in vivo experiment. So, it remains to be seen whether the in vitro rank ordering of ADCs and IVIVC would hold up if different cell lines were used to conduct the analysis. Also, for one of the

ADCs there was no efficacy observed in vitro, however there was a marginal efficacy in vivo. This could occur because the in vitro cell culture medium provides a different biological milieu than the in vivo system, where the chances of an ADC being digested by a different mechanism and locally releasing the payload in the tumor may be a factor. Nonetheless, the ADC with IC50 value of >1000 nM had a very high $TSC_{in\ vivo}$ value as well, implying the weak efficacy in vitro is aptly translated to a weak efficacy in vivo. All the ADCs tested had payloads with similar mechanisms of action, and the IVIVC approach presented here should also be verified using payloads with diverse mechanism of action. Here we have assumed that nominal concentrations of ADC in the media remain the same, however it is well known that payload may fall off ADCs in the media. So, ideally one should account for the decreasing ADC concentrations in the media while modeling the in vitro data, but it becomes too laborious to measure ADC concentrations in all wells at each time point. Hence, we have assumed the constant concentration of ADC in media.

The IVIVC approach established in this manuscript also showcases the tremendous potential of PK/PD modeling in integrating the available in vitro and in vivo data. Without such tools it would not have been possible to integrate all the in vitro and in vivo data to come up with one single variable representing the efficacy of a molecule in each experimental setting, which can be compared with each other to establish IVIVC. It is hypothesized that the methodology to establish IVIVC presented here can be applied to all anticancer therapeutic drugs. Since this approach accounts for in vitro and in vivo PK of the molecules and associates this PK with the observed efficacy of the molecules, it helps in establishing a relationship that purely depends on compounds' potency. Thus, one should be able to establish IVIVC for any class of anticancer agents (e.g. small molecule or large molecule) using any of the available cancer cell lines. However, one has to keep in mind that this approach assumes that the cancer cells behaves similarly during in vitro and in vivo experiments, which may not always be true. One can also conduct the kinetic in vitro experiment with toxicity prone tissue cells (e.g. liver or bone marrow cells) to generate a toxicity matrix similar to $TSC_{in\ vitro}$, which can help in generating an in vitro therapeutic index that could provide a better parameter for triaging anticancer drugs at the discovery stage.

In summary, here we have presented a novel methodology to establish IVIVC for anticancer drugs, which uses PK/PD modeling to integrate the information obtained from the experimental data. The in vitro potency was represented as $TSC_{in\ vitro}$ and the in vivo potency was represented as $TSC_{in\ vivo}$. Data from 19 different ADCs was used to establish the IVIVC between $TSC_{in\ vitro}$ and $TSC_{in\ vivo}$, which provided a very good positive correlation evident from the Spearman's rank correlation coefficient value of 0.82. Establishing IVIVC for oncology drugs provides a tremendous savings in terms of time and resources, along with an ability to triage correct molecules based on their potency in the discovery or early drug development stage. The PK/PD modeling approach to establish IVIVC presented here should be verified by employing a diverse set of anticancer drugs and cell lines.

References

1. Lobo ED, Balthasar JP (2002) Pharmacodynamic modeling of chemotherapeutic effects: application of a transit compartment model to characterize methotrexate effects in vitro. AAPS pharmSci 4 (4):E42. doi:10.1208/ps040442
2. Simeoni M, Magni P, Cammia C, De Nicolao G, Croci V, Pesenti E, Germani M, Poggesi I, Rocchetti M (2004) Predictive pharmacokinetic-pharmacodynamic modeling of tumor growth kinetics in xenograft models after administration of anticancer agents. Cancer research 64 (3):1094-1101
3. Yang J, Mager DE, Straubinger RM (2010) Comparison of two pharmacodynamic transduction models for the analysis of tumor therapeutic responses in model systems. The AAPS journal 12 (1):1-10. doi:10.1208/s12248-009-9155-7
4. Tomayko MM, Reynolds CP (1989) Determination of subcutaneous tumor size in athymic (nude) mice. Cancer chemotherapy and pharmacology 24 (3):148-154
5. Shah DK, Haddish-Berhane N, Betts A (2012) Bench to bedside translation of antibody drug conjugates using a multiscale mechanistic PK/PD model: a case study with brentuximab-vedotin. Journal of pharmacokinetics and pharmacodynamics 39 (6):643-659. doi:10.1007/s10928-012-9276-y
6. Haddish-Berhane N, Shah DK, Ma D, Leal M, Gerber HP, Sapra P, Barton HA, Betts AM (2013) On translation of antibody drug conjugates efficacy from mouse experimental tumors to the clinic: a PK/PD approach. Journal of pharmacokinetics and pharmacodynamics 40 (5):557-571. doi:10.1007/s10928-013-9329-x
7. Fiebig HH, Maier A, Burger AM (2004) Clonogenic assay with established human tumour xenografts: correlation of in vitro to in vivo activity as a basis for anticancer drug discovery. European journal of cancer 40 (6):802-820. doi:10.1016/j.ejca.2004.01.009
8. Johnson JI, Decker S, Zaharevitz D, Rubinstein LV, Venditti JM, Schepartz S, Kalyandrug S, Christian M, Arbuck S, Hollingshead M, Sausville EA (2001) Relationships between drug activity in NCI preclinical in vitro and in vivo models and early clinical trials. British journal of cancer 84 (10):1424-1431. doi:10.1054/bjoc.2001.1796
9. Voskoglou-Nomikos T, Pater JL, Seymour L (2003) Clinical predictive value of the in vitro cell line, human xenograft, and mouse allograft preclinical cancer models. Clinical cancer research : an official journal of the American Association for Cancer Research 9 (11):4227-4239
10. Furukawa T, Kubota T, Watanabe M, Takahara T, Yamaguchi H, Takeuchi T, Kase S, Kodaira S, Ishibiki K, Kitajima M, et al. (1992) High in vitro-in vivo correlation of drug response using sponge-gel-supported three-dimensional histoculture and the MTT end point. International journal of cancer Journal international du cancer 51 (3):489-498

Supplementary Material

Supplementary Table 1: Parameter estimates obtained by fitting the model shown in Figure 1 to the in vitro 'viable cell number vs. time' data generated following incubation of N87 cells with different ADCs.

ADC-1

Parameter	Estimate	%RSE	Unit
Kg	5.93E-01	3	Day^{-1}
$Cell_{Maximum}$	2.13E+05	3	Unit less
Tau_C	0.979	14	Day
Tau_S	0.184	12	Day
$K_{max\_in\_vitro}$	2.49	6	Day^{-1}
$IC^{\gamma}_{50\_in\_vitro}$	0.729	2	nM
γ	1	Fixed	Unit less

ADC-2

Parameter	Estimate	%RSE	Unit
Kg	5.52E-01	4	Day^{-1}
$Cell_{Maximum}$	2.54E+05	6	Unit less
Tau_C	0.55	19	Day
Tau_S	0.162	9	Day
$K_{max\_in\_vitro}$	1.07	0	Day^{-1}
$IC^{\gamma}_{50\_in\_vitro}$	0.474	4	nM
γ	1	Fixed	Unit less

ADC-3

Parameter	Estimate	%RSE	Unit
Kg	3.73E-01	6	Day^{-1}
$Cell_{Maximum}$	3.21E+05	12	Unit less
Tau_C	0.231	24	Day
Tau_S	0.0187	41	Day
$K_{max\_in\_vitro}$	1.17	1	Day^{-1}
$IC^{\gamma}_{50\_in\_vitro}$	1.3	2	nM
γ	1	Fixed	Unit less

ADC-4

Parameter	Estimate	%RSE	Unit
Kg	3.75E-01	6	Day^{-1}
$Cell_{Maximum}$	4.12E+05	15	Unit less
Tau_C	0.36	19	Day
Tau_S	0.0463	11	Day
$K_{max\_in\_vitro}$	1.03	0	Day^{-1}
$IC^{\gamma}_{50\_in\_vitro}$	1.09	1	nM
γ	1	Fixed	Unit less

ADC-5

Parameter	Estimate	%RSE	Unit
Kg	9.66E-01	3	Day^{-1}
$Cell_{Maximum}$	2.33E+05	3	Unit less
Tau_C	0.256	39	Day
Tau_S	0.35	10	Day
$K_{max\_in\_vitro}$	1.72	5	Day^{-1}
$IC^{\gamma}_{50\_in\_vitro}$	0.517	5	nM
γ	1	Fixed	Unit less

ADC-6

Parameter	Estimate	%RSE	Unit
Kg	8.69E-01	3	Day^{-1}
$Cell_{Maximum}$	2.20E+05	2	Unit less
Tau_C	3.60E-01	37	Day
Tau_S	0.341	7	Day
$K_{max\_in\_vitro}$	1.72	8	Day^{-1}
$IC^{\gamma}_{50\_in\_vitro}$	0.907	1	nM
γ	1	Fixed	Unit less

ADC-7

Parameter	Estimate	%RSE	Unit
Kg	8.56E-01	3	Day^{-1}
Cell Maximum	2.55E+04	5	Unit less
Tau_C	1.02	18	Day
Tau_S	0.253	8	Day
$K_{max\_in\_vitro}$	3.01	7	Day^{-1}
$IC^{\gamma}_{50\_in\_vitro}$	2.81	7	nM
γ	1	Fixed	Unit less

ADC-8

Parameter	Estimate	%RSE	Unit
Kg	0.928	3	Day^{-1}
Cell Maximum	26500	3	Unit less
Tau_C	1.06	14	Day
Tau_S	0.201	6	Day
$K_{max\_in\_vitro}$	2.21	3	Day^{-1}
$IC^{\gamma}_{50\_in\_vitro}$	2	6	nM
γ	1	Fixed	Unit less

ADC-9

Parameter	Estimate	%RSE	Unit
Kg	0.843	3	Day^{-1}
Cell Maximum	2.58E+04	3	Unit less
Tau_C	1.05	10	Day
Tau_S	1.38E-01	8	Day
$K_{max\_in\_vitro}$	3.32	5	Day^{-1}
$IC^{\gamma}_{50\_in\_vitro}$	6.42	5	nM
γ	1	Fixed	Unit less

ADC-10

Parameter	Estimate	%RSE	Unit
Kg	3.87E-01	6	Day^{-1}
Cell Maximum	3.71E+05	12	Unit less
Tau_C	0.0351	168	Day
Tau_S	0.0297	16	Day
$K_{max\_in\_vitro}$	0.676	5	Day^{-1}
$IC^{\gamma}_{50\_in\_vitro}$	1.91	10	nM
γ	1	Fixed	Unit less

ADC-11

Parameter	Estimate	%RSE	Unit
Kg	4.81E-01	7	Day^{-1}
Cell Maximum	4.44E+04	9	Unit less
Tau_C	1.78E-01	19	Day
Tau_S	0.0434	34	Day
$K_{max\_in\_vitro}$	1.14	2	Day^{-1}
$IC^{\gamma}_{50\_in\_vitro}$	3.25	12	nM
γ	1	Fixed	Unit less

ADC-12

Parameter	Estimate	%RSE	Unit
Kg	0.984	4	Day^{-1}
Cell Maximum	2.80E+04	3	Unit less
Tau_C	2.22E-01	60	Day
Tau_S	2.69E-01	18	Day
$K_{max\_in\_vitro}$	1.51E+00	3	Day^{-1}
$IC^{\gamma}_{50\_in\_vitro}$	2.18E+00	8	nM
γ	1	Fixed	Unit less

ADC-13

Parameter	Estimate	%RSE	Unit
Kg	6.31E-01	3	Day^{-1}
$Cell_{Maximum}$	3.81E+05	3	Unit less
Tau_C	0.347	27	Day
Tau_S	0.224	6	Day
$K_{max\_in\_vitro}$	0.857	2	Day^{-1}
$IC^{\gamma}_{50\_in\_vitro}$	1.68	3	nM
γ	1	Fixed	Unit less

ADC-14

Parameter	Estimate	%RSE	Unit
Kg	1.05	4	Day^{-1}
$Cell_{Maximum}$	25300	4	Unit less
Tau_C	0.199	43	Day
Tau_S	0.302	9	Day
$K_{max\_in\_vitro}$	1.62	3	Day^{-1}
$IC^{\gamma}_{50\_in\_vitro}$	3.04	8	nM
γ	1	Fixed	Unit less

ADC-15

Parameter	Estimate	%RSE	Unit
Kg	1	3	Day^{-1}
$Cell_{Maximum}$	2.57E+04	4	Unit less
Tau_C	1.58E+00	15	Day
Tau_S	0.0564	11	Day
$K_{max\_in\_vitro}$	1.23	1	Day^{-1}
$IC^{\gamma}_{50\_in\_vitro}$	2.79	9	nM
γ	1	Fixed	Unit less

ADC-16

Parameter	Estimate	%RSE	Unit
Kg	5.05E-01	3	Day^{-1}
$Cell_{Maximum}$	2.54E+05	5	Unit less
Tau_C	0.747	18	Day
Tau_S	0.0928	12	Day
$K_{max\_in\_vitro}$	0.731	1	Day^{-1}
$IC^{\gamma}_{50\_in\_vitro}$	6.83	4	nM
γ	1	Fixed	Unit less

ADC-17

Parameter	Estimate	%RSE	Unit
Kg	5.99E-01	3	Day^{-1}
$Cell_{Maximum}$	3.68E+05	3	Unit less
Tau_C	0.488	22	Day
Tau_S	0.197	11	Day
$K_{max\_in\_vitro}$	0.73	4	Day^{-1}
$IC^{\gamma}_{50\_in\_vitro}$	5.74	9	nM
γ	1	Fixed	Unit less

ADC-18

Parameter	Estimate	%RSE	Unit
Kg	6.12E-01	2	Day^{-1}
$Cell_{Maximum}$	3.70E+05	2	Unit less
Tau_C	0.436	35	Day
Tau_S	0.226	22	Day
$K_{max\_in\_vitro}$	0.72	2	Day^{-1}
$IC^{\gamma}_{50\_in\_vitro}$	5.23	6	nM
γ	1	Fixed	Unit less

Supplementary Table 2: Parameter estimates obtained by fitting the model shown in Figure-2 to the TGI data generated in N87 xenografts following administration of different ADCs.

ADC-1

Parameter	Estimate	%RSE	Unit
$k_{g\ Exponential}$	0.102	7	Day^{-1}
$k_{gLinear}$	28.6	9	$mm^3 \bullet Day^{-1}$
V_{Max}	4.16E+03	22	mm^3
Tau	1.68	6	Day
k_{kill_Max}	0.174	4	Day^{-1}
KC_{50}	1.01	0	µg/mL
ψ	20	Fixed	Unit less
$IIV\_k_{g\ Exponential}$	0.266	94	Unit less
$IIV\_k_{g\ Linear}$	0.393	23	Unit less

ADC-2

Parameter	Estimate	%RSE	Unit
$k_{g\ Exponential}$	0.0745	6	Day^{-1}
$k_{gLinear}$	51.8	14	$mm^3 \bullet Day^{-1}$
V_{Max}	2.01E+03	8	mm^3
Tau	1.34	7	Day
k_{kill_Max}	0.212	6	Day^{-1}
KC_{50}	3.04	17	µg/mL
ψ	20	Fixed	Unit less
$IIV\_k_{g\ Exponential}$	0.222	70	Unit less
$IIV\_k_{g\ Linear}$	0.478	23	Unit less

ADC-3

Parameter	Estimate	%RSE	Unit
$k_{g\ Exponential}$	0.138	7	Day^{-1}
$k_{gLinear}$	58.5	8	$mm^3 \bullet Day^{-1}$
V_{Max}	3.82E+03	17	mm^3
Tau	5.01	2	Day
k_{kill_Max}	0.585	1	Day^{-1}
KC_{50}	15.9	7	µg/mL
ψ	20	Fixed	Unit less
$IIV\_k_{g\ Exponential}$	0.186	58	Unit less
$IIV\_k_{g\ Linear}$	0.322	23	Unit less

ADC-4

Parameter	Estimate	%RSE	Unit
$k_{g\ Exponential}$	0.236	7	Day^{-1}
$k_{gLinear}$	64.3	8	$mm^3 \bullet Day^{-1}$
V_{Max}	3.05E+03	10	mm^3
Tau	3.22	3	Day
k_{kill_Max}	0.975	0	Day^{-1}
KC_{50}	59	8	µg/mL
ψ	20	Fixed	Unit less
$IIV\_k_{g\ Exponential}$	0.349	>100	Unit less
$IIV\_k_{g\ Linear}$	0.357	24	Unit less

ADC-5

Parameter	Estimate	%RSE	Unit
$k_{g\ Exponential}$	0.0636	13	Day^{-1}
$k_{gLinear}$	61.4	18	$mm^3 \bullet Day^{-1}$
V_{Max}	3.95E+03	5	mm^3
Tau	1	0	Day
k_{kill_Max}	0.135	6	Day^{-1}
KC_{50}	2.39	26	µg/mL
ψ	20	Fixed	Unit less
$IIV\_k_{g\ Exponential}$	0.467	28	Unit less
$IIV\_k_{g\ Linear}$	0.548	24	Unit less

ADC-6

Parameter	Estimate	%RSE	Unit
$k_{g\ Exponential}$	0.0982	14	Day^{-1}
$k_{gLinear}$	23.2	12	$mm^3 \bullet Day^{-1}$
V_{Max}	4.68E+03	45	mm^3
Tau	3.44	6	Day
k_{kill_Max}	0.537	17	Day^{-1}
KC_{50}	37.9	22	µg/mL
ψ	20	Fixed	Unit less
$IIV\_k_{g\ Exponential}$	0.34	62	Unit less
$IIV\_k_{g\ Linear}$	0.54	24	Unit less

ADC-7

Parameter	Estimate	%RSE	Unit
$k_{g\ Exponential}$	0.111	5	Day^{-1}
$k_{gLinear}$	64.8	9	$mm^3 \bullet Day^{-1}$
V_{Max}	3.77E+03	33	mm^3
Tau	2.63	6	Day
k_{kill_Max}	0.308	8	Day^{-1}
KC_{50}	11.6	17	µg/mL
ψ	20	Fixed	Unit less
$IIV\_k_{g\ Exponential}$	0.114	>100	Unit less
$IIV\_k_{g\ Linear}$	0.359	26	Unit less

ADC-8

Parameter	Estimate	%RSE	Unit
$k_{g\ Exponential}$	0.138	5	Day^{-1}
$k_{gLinear}$	61.6	8	$mm^3 \bullet Day^{-1}$
V_{Max}	3.77E+03	33	mm^3
Tau	3.94	5	Day
k_{kill_Max}	0.292	7	Day^{-1}
KC_{50}	6.9	19	µg/mL
ψ	20	Fixed	Unit less
$IIV\_k_{g\ Exponential}$	0.114	>100	Unit less
$IIV\_k_{g\ Linear}$	0.359	26	Unit less

ADC-9

Parameter	Estimate	%RSE	Unit
$k_{g\ Exponential}$	0.16	16	Day^{-1}
$k_{gLinear}$	48.7	13	$mm^3 \bullet Day^{-1}$
V_{Max}	5.01E+03	26	mm^3
Tau	5.11	5	Day
k_{kill_Max}	0.265	13	Day^{-1}
KC_{50}	7.36	23	µg/mL
ψ	20	Fixed	Unit less
$IIV\_k_{g\ Exponential}$	0.715	50	Unit less
$IIV\_k_{g\ Linear}$	0.553	23	Unit less

ADC-10

Parameter	Estimate	%RSE	Unit
$k_{g\ Exponential}$	0.254	15	Day^{-1}
$k_{gLinear}$	79.7	8	$mm^3 \bullet Day^{-1}$
V_{Max}	2.77E+03	12	mm^3
Tau	2.84	8	Day
k_{kill_Max}	0.403	29	Day^{-1}
KC_{50}	59.9	45	µg/mL
ψ	20	Fixed	Unit less
$IIV\_k_{g\ Exponential}$	0.594	>100	Unit less
$IIV\_k_{g\ Linear}$	0.359	24	Unit less

ADC-11

Parameter	Estimate	%RSE	Unit
$k_{g\ Exponential}$	0.113	13	Day^{-1}
$k_{gLinear}$	61.5	9	$mm^3 \bullet Day^{-1}$
V_{Max}	4.38E+03	16	mm^3
Tau	1.1	16	Day
k_{kill_Max}	0.236	25	Day^{-1}
KC_{50}	189	40	µg/mL
ψ	20	Fixed	Unit less
$IIV\_k_{g\ Exponential}$	0.575	31	Unit less
$IIV\_k_{g\ Linear}$	0.45	24	Unit less

ADC-12

Parameter	Estimate	%RSE	Unit
$k_{g\ Exponential}$	0.12	9	Day^{-1}
$k_{gLinear}$	31.4	8	$mm^3 \bullet Day^{-1}$
V_{Max}	4.19E+03	23	mm^3
Tau	4.41	4	Day
k_{kill_Max}	0.78	0	Day^{-1}
KC_{50}	86.6	5	µg/mL
ψ	20	Fixed	Unit less
$IIV\_k_{g\ Exponential}$	0.365	75	Unit less
$IIV\_k_{g\ Linear}$	0.382	23	Unit less

ADC-13

Parameter	Estimate	%RSE	Unit
$k_{g\ Exponential}$	0.11	20	Day^{-1}
$k_{gLinear}$	23.4	14	$mm^3 \bullet Day^{-1}$
V_{Max}	4.37E+03	7	mm^3
Tau	3.44	6	Day
k_{kill_Max}	0.148	18	Day^{-1}
KC_{50}	21.8	44	µg/mL
ψ	20	Fixed	Unit less
$IIV\_k_{g\ Exponential}$	0.5	Fixed	Unit less
$IIV\_k_{g\ Linear}$	0.791	24	Unit less

ADC-14

Parameter	Estimate	%RSE	Unit
$k_{g\ Exponential}$	0.0732	11	Day^{-1}
$k_{gLinear}$	37.9	17	$mm^3 \bullet Day^{-1}$
V_{Max}	4.22E+03	18	mm^3
Tau	1.36	16	Day
k_{kill_Max}	0.405	38	Day^{-1}
KC_{50}	131	48	µg/mL
ψ	20	Fixed	Unit less
$IIV\_k_{g\ Exponential}$	0.47	38	Unit less
$IIV\_k_{g\ Linear}$	0.781	27	Unit less

ADC-15

Parameter	Estimate	%RSE	Unit
$k_{g\ Exponential}$	0.219	18	Day^{-1}
$k_{gLinear}$	15.9	26	$mm^3 \bullet Day^{-1}$
V_{Max}	2.27E+03	14	mm^3
Tau	0.999	29	Day
k_{kill_Max}	0.126	42	Day^{-1}
KC_{50}	52.3	91	µg/mL
ψ	20	Fixed	Unit less
$IIV\_k_{g\ Exponential}$	0.182	>100	Unit less
$IIV\_k_{g\ Linear}$	1.22	23	Unit less

ADC-16

Parameter	Estimate	%RSE	Unit
$k_{g\ Exponential}$	0.0934	8	Day^{-1}
$k_{gLinear}$	38.1	13	$mm^3 \bullet Day^{-1}$
V_{Max}	3.42E+03	21	mm^3
Tau	2.52	15	Day
k_{kill_Max}	0.225	55	Day^{-1}
KC_{50}	177	84	µg/mL
ψ	20	Fixed	Unit less
$IIV\_k_{g\ Exponential}$	0.283	39	Unit less
$IIV\_k_{g\ Linear}$	0.748	26	Unit less

ADC-17

Parameter	Estimate	%RSE	Unit
$k_{g\ Exponential}$	0.0844	12	Day^{-1}
$k_{gLinear}$	54.9	12	$mm^3 \bullet Day^{-1}$
V_{Max}	4.24E+03	21	mm^3
Tau	0.999	5	Day
k_{kill_Max}	0.175	25	Day^{-1}
KC_{50}	70.9	48	µg/mL
ψ	20	Fixed	Unit less
$IIV\_k_{g\ Exponential}$	0.483	27	Unit less
$IIV\_k_{g\ Linear}$	0.516	24	Unit less

ADC-18

Parameter	Estimate	%RSE	Unit
$k_{g\ Exponential}$	0.266	12	Day^{-1}
$k_{gLinear}$	81.4	10	$mm^3 \bullet Day^{-1}$
V_{Max}	2.57E+03	9	mm^3
Tau	6.36	5	Day
k_{kill_Max}	0.353	3	Day^{-1}
KC_{50}	14.5	10	µg/mL
ψ	20	Fixed	Unit less
$IIV\_k_{g\ Exponential}$	0.533	>100	Unit less
$IIV\_k_{g\ Linear}$	0.479	23	Unit less

ADC-19

Parameter	Estimate	%RSE	Unit
$k_{g\ Exponential}$	0.133	10	Day^{-1}
$k_{gLinear}$	70.6	12	$mm^3 \bullet Day^{-1}$
V_{Max}	5.19E+03	20	mm^3
Tau	0.819	22	Day
k_{kill_Max}	0.192	14	Day^{-1}
KC_{50}	75.7	29	µg/mL
ψ	20	Fixed	Unit less
$IIV\_k_{g\ Exponential}$	0.402	29	Unit less
$IIV\_k_{g\ Linear}$	0.657	23	Unit less